

Cleavage Furrow Formation for Avascular Tumor Growth based on Finite Element Modeling

Changyu Liu¹, Dapeng Li^{2*}, Bin Lu³ and Tiezhu Zhao⁴

¹*School of Computer Science and Engineering, South China University of Technology, Guangzhou 510006, China*

²*College of Telecommunications and Information Engineering, Nanjing University of Posts and Telecommunications, Nanjing 210003, China*

³*School of Computer Science, Wuyi University, Jiangmen 529020, China*

⁴*Computer College, Dongguan University of Technology, Dongguan 523808, China*
*yezhigh@gmail.com, *dapengli@njupt.edu.cn (corresponding author), lbscut@gmail.com, tzzhao83@163.com*

Abstract

A number of studies have shown that the prevention and cure of malignant tumors may become much easier if growth mechanisms, such as the role of cleavage furrow formation in tumor cell division, could be discovered and understood in the earlier avascular phase. Although it is well known that metazoan mitotic spindle which is one of the most important substances during the cytokinesis of a cell division determines the position of the cleavage furrow formation, we are still on the verge of solving the puzzle of what molecules and how they control the formation of the cleavage furrow. In this paper, we propose a cleavage furrow formation approach based on finite element method, which combines nodes selection, mesh partition and matrix assembly in a total energy equation, for modeling the mechanisms of avascular tumor growth. We also perform several experiments. Results show that, by using our proposed approach for the avascular tumor growth, the positions of cleavage furrows are decided not only chemically but also physically and tumor cells are not symmetric, which demonstrates the effectiveness of our proposed approach.

Keywords: *cleavage furrow formation, cell division, finite element, avascular tumor growth*

1. Introduction

The occurrence of malignant tumors is an extremely complex biological phenomena that composed of several stages with multiple factors interaction and polygene participation. In the early seventies, Folkman *et al.*, considered the growth of the solid tumor to be two separate phases, which are an avascular phase and a vascular phase [1]. With a more comprehensive research, it is widely considered that there are three phases during the tumor growth, which are an avascular tumor growth phase, an angiogenesis phase and a vascular tumor growth phase [3].

In the first avascular phase, the tumor spheroid grows without special blood vessels. All the needed nutrients are provided by diffusions from their surrounding tissues. The tumor spheroid undergoes a further saturated growth after the earlier exponential growth due to the limited nutrients [5]. The tumor spheroid diameter is about one to two millimeter [7] and the cell size is about 10^6 in this phase. In the second angiogenesis phase, many inducing factors, such as vascular endothelial growth factor (also called VEGF), are released to their surrounding host tissues by cancerous cells. These factors could activate some proteins genes which could control the growth of new blood vessels. After the formation of new tumor vessels, the tumor growth enters the third vascular

phase. The nutrients for large scale tumor growth are provided by the rapidly increased vessels, causing an unrestricted growth. Tumor cells in this phase can also circulate with blood and invade many remote normal tissues. Therefore, if the growth mechanism could be discovered and understood in the earlier avascular phase, the prevention and cure of such malignant tumors may become more easier.

Although researches, such as [9, 11, 13], have shown that the spindle plays a key role not only in bringing about the mechanical separation of chromosomes, but also in determining the position of the cleavage furrow in animal cells, the exact nature of this role, such as whether spindle inhibits furrow formation close to the spindle poles or delivers a inducing signal of furrow formation at the equatorial cortex, has been debated. In this paper, we proposed a finite element based cleavage furrow formation approach, which tries to understand the mechanisms of avascular tumor growth not only from the chemical aspect, such as modeling the role of cell cycle control factors and reaction diffusion substances, but also from the physical aspect, such as modeling the role of cell surface and cell volume. We also proved the effectiveness of our proposed approach by several experiments.

2. Finite Element Based Modeling

In order to understand how the cleavage furrow formation process contributes to the growth of avascular tumor which is based on Eq. (10) of paper [15], the finite element based modeling approaches, which include nodes selection, mesh partition and matrix assembly, should be adopted firstly to construct the needed physical structure data for solving these equations.

2.1. Nodes Selection

The first step for a FEM based physical modeling is to select nodes that would be used for further simulation. In order to get the offset of each node after its growth, we use four data structures which are defined as follows to record the physical information for the tumor growth.

Definition 1 (Node Structure). A node structure is defined as: `typedef struct {double x; double y; double z;} node, *nodeptr;` where x, y, z are three dimension double-precision floating-point coordinates.

Definition 2 (Edge Structure). An edge structure is defined as: `typedef struct {int NL[2];}edge, *edgeptr;` where NL is an integer array that composes of two ordinal nodes in an edge.

Definition 3 (Element Structure). An element structure (also called mesh surface structure) is defined as: `typedef struct {int ALN[3];} element, *elementptr;` where ALN is an integer array that composes of three sequential global identifiers for nodes in a triangle according to the right hand rule.

Definition 4 (Cell Structure). A cell structure is defined as: `typedef struct{vector<int> AL; vector<int> NL_C2G; int node_num;}cell;` where `node_num` is the nodes number of one tumor cell, AL is the numbered integer element array, NL_C2G is used to transfer the local cell identifier to the global identifier with `NL_C2G[i] == j` meaning that the global number of i node in one cell is j .

In order to use the FEM method to get the Node Structure data, each tumor cell is treated as a standard sphere and triangular surface grids are established to represent the tumor cell surface. The more triangular surfaces we obtain, the more accurate tumor growth results we will get then. This can be seen in Figure 1. In our preliminary experiment, we take into account separately 6 nodes, 10 nodes, and 18 nodes in early experiments. After that, we use 152 nodes.

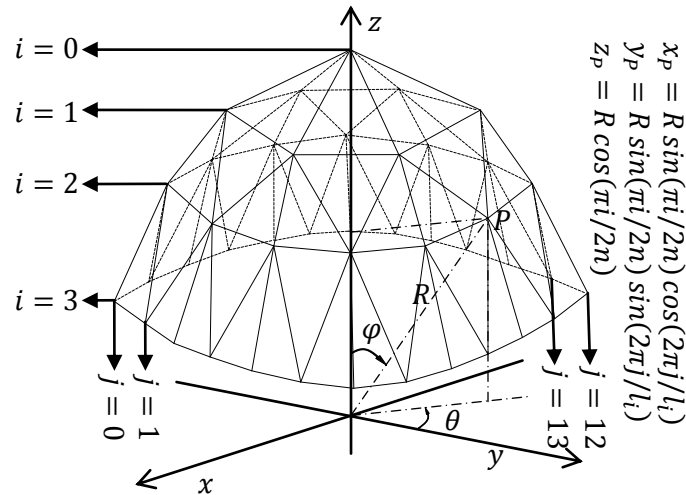


Figure 1. Parameter Structure of Sphere Surface

The center of a sphere represents the cell center. The sphere is divided to $2n$ equal proportions along the latitude direction which has range of $\varphi \in [0, \pi]$. The spherical coordinates can be expressed by parameter equations as:

$$x = R \sin \varphi \cos \theta \quad y = R \sin \varphi \sin \theta \quad z = R \cos \varphi \quad (1)$$

Firstly, we set the dividing layer of a half tumor sphere to be n and of a whole tumor sphere to be $2n$. In Figure 1, n equates 4, 0 means the Arctic layer and $2n$ means the Antarctic layer. Then, each layer is divided into several nodes with one node for two poles and a more 6 nodes for the later layer to the equator direction. The node number of the i -th layer is $l_i = 6 \times (n - |n - i|)$. The expression of φ and θ will be got from Figure 1, as:

$$\varphi = \pi/2n \quad \theta = 2\pi/l_i \quad (2)$$

Finally, each node coordinate could be obtained as follows, where i is the layer number, j is the latitude number.

$$\varphi_{NL} = \pi i/2n \quad \theta_{NL} = 2\pi j/l_i \quad (3)$$

2.2. Mesh Partition

After the above nodes selection, the node structure data is obtained. The following work is to get the edge structure data and the element structure data through a mesh partition approach. In order to use the popular Delaunay triangulation algorithm, the partition for mesh nodes should meet an empty circle characteristics principle, which is defined as: (1) Any four nodes must not share a circle in the Delaunay triangulation. (2) The circumcircle of any triangle must not contain any other vertices. In this paper, we use the Bowyer Watson algorithm, which adopts the following steps to meet the empty circle characteristics principle for a Delaunay triangulation. This can be seen from Figure 2.

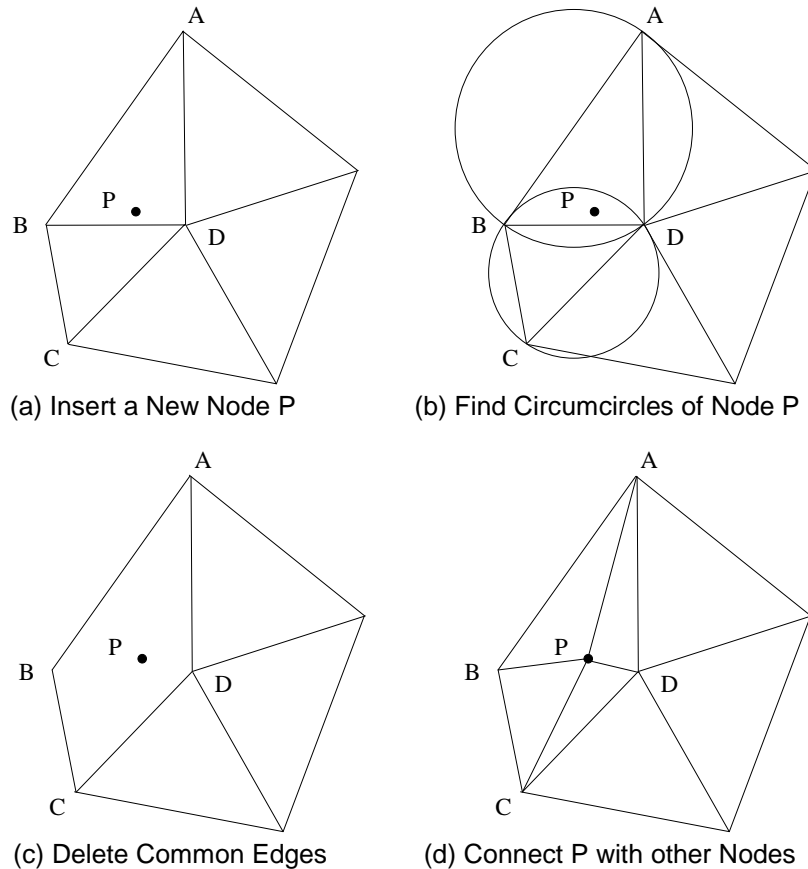


Figure 2. Delaunay Triangulation for New Node P According to the Empty Circle Characteristics Principle

As such, a detailed Delaunay triangulation process contains: (1) Divide the whole sphere into two hemispheres that are a southern Hemisphere with $z \leq 0$ and a Northern Hemisphere with $z \geq 0$. (2) Map the hemisphere nodes into the XY surface. (3) Construct three nodes to form a triangle which could contain all the mapped nodes. (4) Add one new node each time from the mapped nodes set to the already existed mesh surface according to the previous method from Figure 2. (5) Determine which triangles contain the new added nodes. (6) Delete the common edges among the shared triangles. (7) Connect all nodes of shared triangles with this new added node to form new triangles. (8) Jump to execute step 4 until there is no one node in the mapped nodes set. (9) Delete the initial three nodes and the related edges.

2.3. Matrix Assembly

After the above steps, the data of node structure, edge structure and the element structure are obtained. The following work is to get the cell structure data. Here a matrix assembly method is proposed in this paper. The solving of total energy equation is to compute three offsets that are u for x axis, v for y axis and w for z axis of all nodes. If NN nodes are selected, the final equation solving results contain $3*NN$ value. Thus, the K is a $(3*NN, 3*NN)$ matrix and F is a $3*NN$ column vector. According to Eq. (10) of paper [15], the $[K_S]_A$ is a $9*9$ matrix, while both $\{F_S\}_A$ and $\{F_V\}_C$ are a 9 dimension column vector. Due to the fact that K and F are composed of $\{F_S\}_A$, $[K_S]_A$ and $\{F_V\}_C$, a matrix and vector assembly is needed for these transforms. Take $\{F_S\}_A$ for example, we describe how to realize the matrix assembly function as follows. Firstly, $\{F_S\}_A$ is obtained from the element structure which has three sequential nodes N_1 , N_2 and N_3 . Thus, there

are 9 value, which are x_1, y_1 and z_1 for N_1 , x_2, y_2 and z_2 for N_2 and x_3, y_3 and z_3 for N_3 in $\{F_S\}_A$. This transform can be marked with i ($0 \leq i < 3$) and j ($0 \leq j < 3$), where i is the sequence number of current node which has a global identifier Elem.ALN[i] in the element structure, j is the offset of this node with value 0 denotes from x axis, 1 from y axis and 2 from z axis. So, it is only needed to find the position Elem.ALN[i] in global vector $\{F_S\}_{Global}$ and substitute it with $i * 3 + j$ to get Elem.ALN[i]*3+ j for $\{F_S\}_{Global}$.

Figure 3 shows how to assembly the local $[K_S]$ to form the global $[K_S]_{Global}$. Due to the $[K_S]$ is a 9*9 matrix, we can divide it into nine 3*3 matrix and map each 3*3 matrix to the appropriate global position. For example, we can map the local number (N_1, N_2) of left dark 3*3 matrix to global (Elem.ALN[1], Elem.ALN[2]) and move these value to corresponding positions. After these steps, cell structure is obtained.

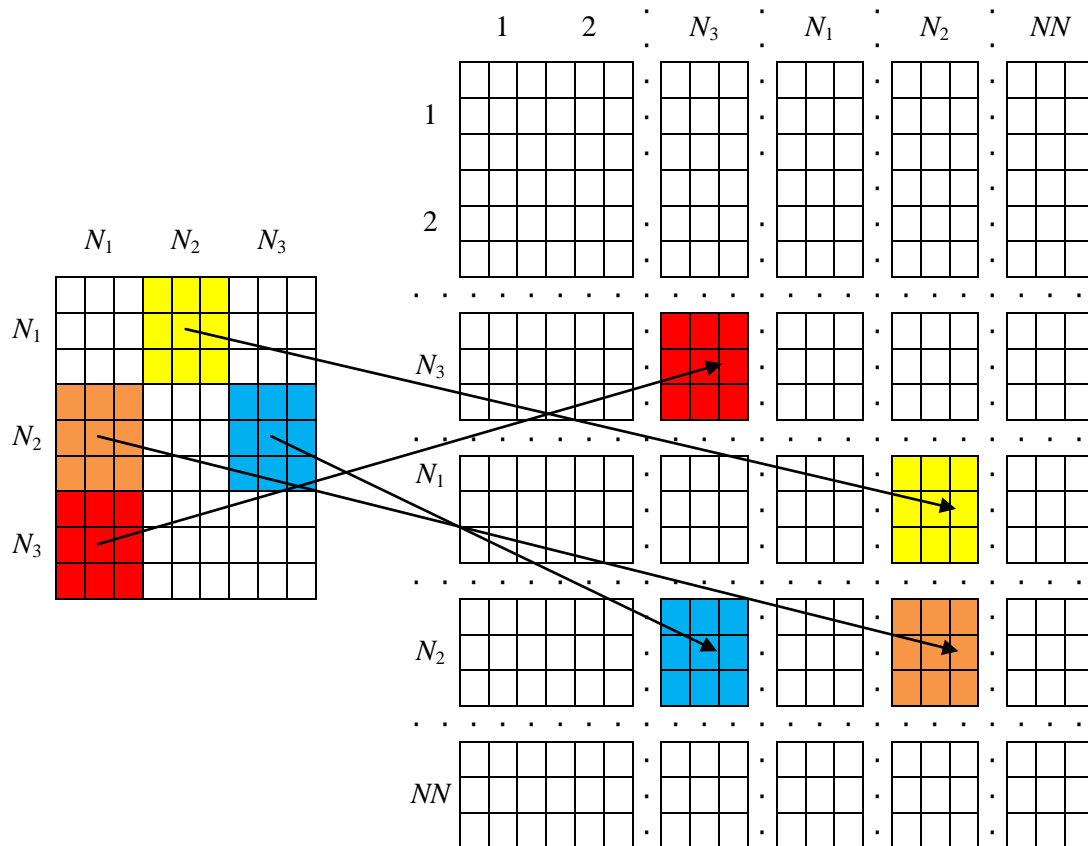


Figure 3. Matrix Assembly

3. Cleavage Furrow Formation

The growth of avascular tumor spheroid is inhibited due to the limited nutrients that are obtained only from the diffusion effect on its surface. When the total cell energy, as shown in Eq. (3) of paper [15], drops to a critical point as a result of the increase of cell volume and cell surface area, one single cell may be divided into several cells. Since we get the basic data for our physical growth simulation, we can then solve the total energy equation by using a LU decomposition approach to determine when it grows to a critical status that a tumor cell should be divided. But we still need to know how to form the shape and position of a division plane, which is also called cleavage furrow, because a proper position of the cell division plane during mitosis is essential for determining the size and position of two daughter cells.

According to [17], division always occurs at a cortical position that is distal to the chromosomes and is controlled by factors from chromosomes which activate a subpopulation of stable microtubules not only to extend through chromosomes but also to bind to the cell cortex at the site of furrow formation. In this paper, we proposed a cell cycle control factor $F(\vec{x}, t)$ that played a same role as a proteins list [19] in the whole tumor cell cycles, where $\vec{x} = (x, y, z)^T$ is a three dimension coordinates vector and t is the tumor growth time. In our model, we substitute mesh grids of the division plane for microtubules and the local factor level $F(\vec{x}, t)$ for the factors from chromosomes due to their similarities. The next step is focused on how to get the mesh grids of a division plane.

Let $\{x_1, y_1, z_1\}, \{x_2, y_2, z_2\}, \dots, \{x_n, y_n, z_n\}$ be n surface points in the bounded closed domain Ω of object, then the areal coordinate $P_0 = \{x_0, y_0, z_0\}$ of this object is,

$$x_0 = \frac{1}{n} \sum_{i=1}^n x_i \quad y_0 = \frac{1}{n} \sum_{i=1}^n y_i \quad z_0 = \frac{1}{n} \sum_{i=1}^n z_i \quad (4)$$

In our model, $\{x_n, y_n, z_n\}$ is the n -th node in the previous computed cell structure, the gradient descent direction of $F(\vec{x}, t)$ at P_0 is taken as the normal vector \vec{n} of division plane Π_0 that decided by the chromosomes with

$$\vec{n} = (\xi_1, \xi_2, \xi_3) = \nabla\{F(\vec{x}, t)\} = \left(\frac{\partial F}{\partial x}, \frac{\partial F}{\partial y}, \frac{\partial F}{\partial z} \right) \quad (5)$$

and the division plane Π_0 can be constructed with a point-normal form equation of a plane that crosses the areal coordinates P_0 , as:

$$\xi_1(x - x_0) + \xi_2(y - y_0) + \xi_3(z - z_0) = 0 \quad (6)$$

Due to the distance from a point $P_i = \{x_i, y_i, z_i\}$ to a plane $\Pi_1: Ax + By + Cz + D = 0$ is

$$d_i = \frac{|Ax_i + By_i + Cz_i + D|}{\sqrt{A^2 + B^2 + C^2}} \quad (7)$$

we can substitute Π_0 for Π_1 and get the distance d_i between a cell surface point and its areal coordinates P_0 , as:

$$d_i = \frac{|(\xi_1 x_i + \xi_2 y_i + \xi_3 z_i) - (\xi_1 x_0 + \xi_2 y_0 + \xi_3 z_0)|}{\sqrt{\xi_1^2 + \xi_2^2 + \xi_3^2}} \quad (8)$$

The boundary of division plane consists of nodes P_i that meet $d_i \leq d_0$, where d_0 is the threshold. The following steps show a division plane formation process that combines an internal nodes construction and a mesh partition, which are:

(1) Find all edges that exist within the division plane boundary from the edge structure and divide the tumor cell point set $V = \{v_i\}$ together with edge set $E = \{e_i\}$ into two daughter cells point sets $V = \{V_1, V_2\}$ and edge sets $E = \{E_1, E_2\}$, according to boundary vertices.

(2) If the boundary edge sets are composed of N separate connected components, new N edges are constructed to connect these components to form a closed loop boundary according to the principle of the minimum distance between two separately connected components.

(3) Select any boundary point to be a starting point and divide the edges of the closed loop boundary into n groups that start from this point and consist of three consecutive edges except the last group which may contain edge number of $\emptyset_n \in \{1,2,3\}$. These external n grouping nodes are marked as L_i and the internal nodes between L_i and L_{i+1} are marked as L_{ij} , where $i \in \{0,1, \dots, n\}$ and $j \in \{1,2\}$.

(4) Connect the areal coordinate c with L_i and separate cL_i into three equal sections.

(5) Connect successively firstly the nodes that have a distance of $cL_i/3$ from the areal coordinate c and secondly the nodes that have a distance of $2cL_i/3$ from the areal coordinate c . On the $2cL_i/3$ circle, add new nodes in the center of each edge for these groups if the edge number of i group $\emptyset_i = 3$ and do nothing if $\emptyset_i \in \{1,2\}$.

(6) Connect successively each new added nodes (also middle nodes) in the $2cL_i/3$ circle with two neighbor internal nodes L_{ij} from external closed loop boundary and connect each of these L_{ij} with non-internal neighbor nodes in the $2cL_i/3$ circle. After these steps, a mesh surface of division plane is obtained.

(7) Add these new nodes and edges into V_1, V_2 and E_1, E_2 to form two daughter cells.

4. Multi-cellular Tumor Growth

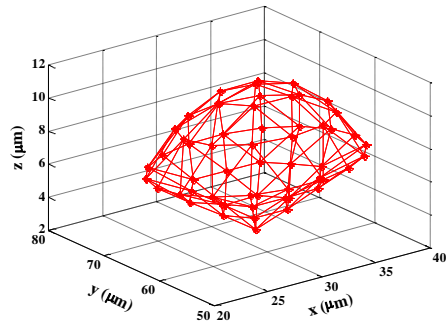
After the formation of cleavage furrow, one tumor cell will become two daughter cells if it meets the division condition. Thus, the physical tumor growth would enter a multi-cellular phase which is more or less the same as the single cellular growth. It needs also to compute the total stiffness matrices $[K]$ and the vector $\{F\}$ according the same energy equation. The whole process follows the same four steps as that of the single-cellular tumor growth, which are nodes selection, mesh partition, matrix assembly and cleavage furrow formation. The main difference here lies in the computing of $\{F_V\}_{AL_C}$ and $\{F_V\}_C$. To the multi-cellular tumor growth, the assembly of $\{F_V\}_{AL_C}$ and $\{F_V\}_C$ is more locally.

It can be seen from Eq. (10) of paper [15] that the global $\{F_V\}_C$ can be only obtained after the computing of local $\{F_V\}_C$. Let n be the nodes number in one cell, m be the total nodes number for a tumor spheroid. The total computing and assembly process is as: (1) Compute a 9 dimension vector $\{F_V\}_{AL_C}$ according to one specific triangle element structure. (2) Assemble this local vector $\{F_V\}_{AL_C}$ of one cell to $3n$ dimension vector $\{F_V\}_C$, and obtain a $3n * 3n$ temporary matrix according to the vector multiplication of $\{F_V\}_C \{F_V\}_C^T$. (3) Assemble the temporary $3n * 3n$ matrix to form a global $3m * 3m$ matrix according to the relationship between the local cell and the global spheroid. The key step lies in the matrix assembly method we discuss before.

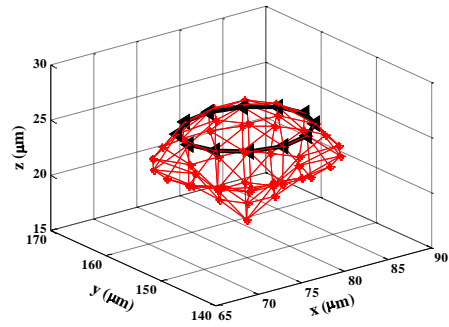
5. Experiments

For physical tumor growth, we firstly construct an initial cell at the origin by using the FEM method of Figure 1, where we set model parameters at: $radius = 11.2725 \mu m$, $node number = 152$, $mesh number = 300$, $center = origin$, and $status = P$. Then, we use these initialized data to simulate the cleavage furrow formation for the physical tumor growth under chemical concentrations of 0.08mM oxygen, 5.5mM glucose, 0mM GIF.

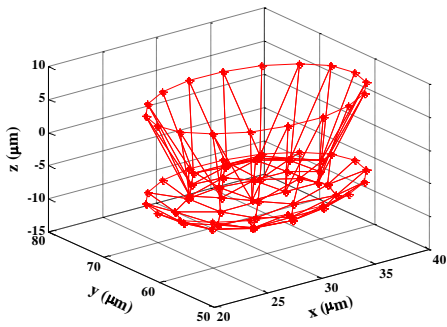
Figure 4 and Figure 5 show results of cleavage furrow formation for the physical tumor growth. The format of all figure names are $(xy-z)$, where $x \in \{a,b\}$ refers to the cell division level, a and b represent separately the second time and the third time division of a tumor cell, y refers to the cell id in the cell division level of x , $z = 1$ means that a cell xy does not have a growth in the current level, and $z = 2$ means that a cleavage furrow boundary is formed after a FEM growth from the cell $xy -1$, as shown with black cycles in Figure 4 and Figure 5.



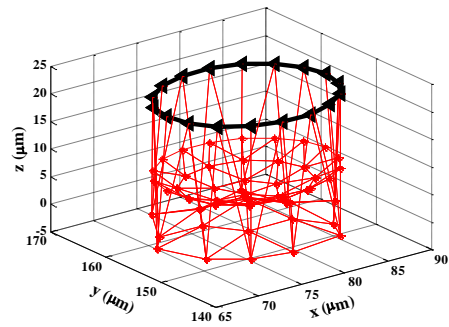
(a1-1)



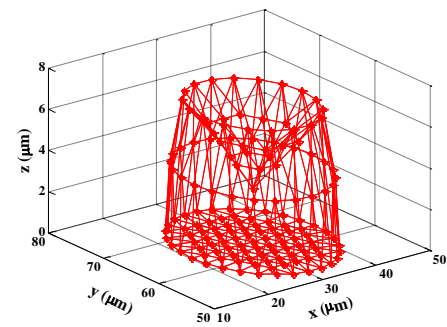
(a1-2)



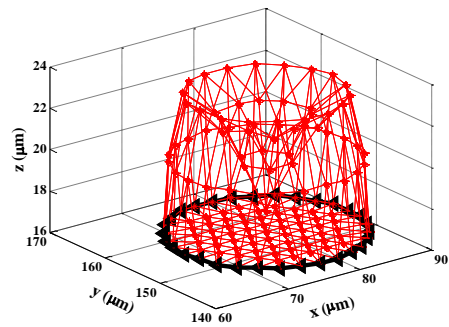
(a2-1)



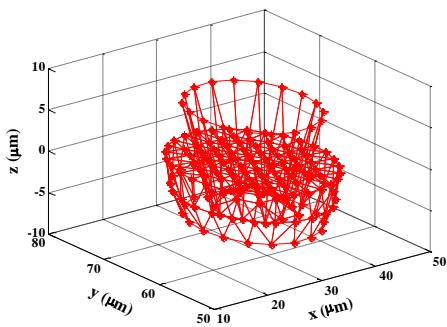
(a2-2)



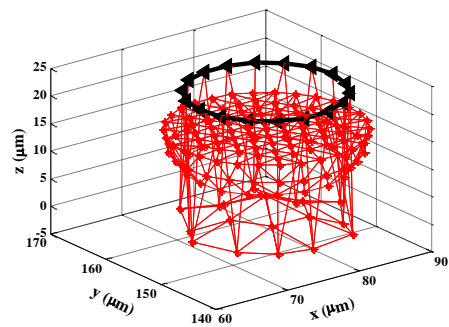
(a3-1)



(a3-2)



(a4-1)



(a4-2)

Figure 4. Results of Cleavage Furrow Formation for Four Cells from the Second Time Division under 0.08 mM oxygen, 5.5 mM Glucose and 0 mM GIF

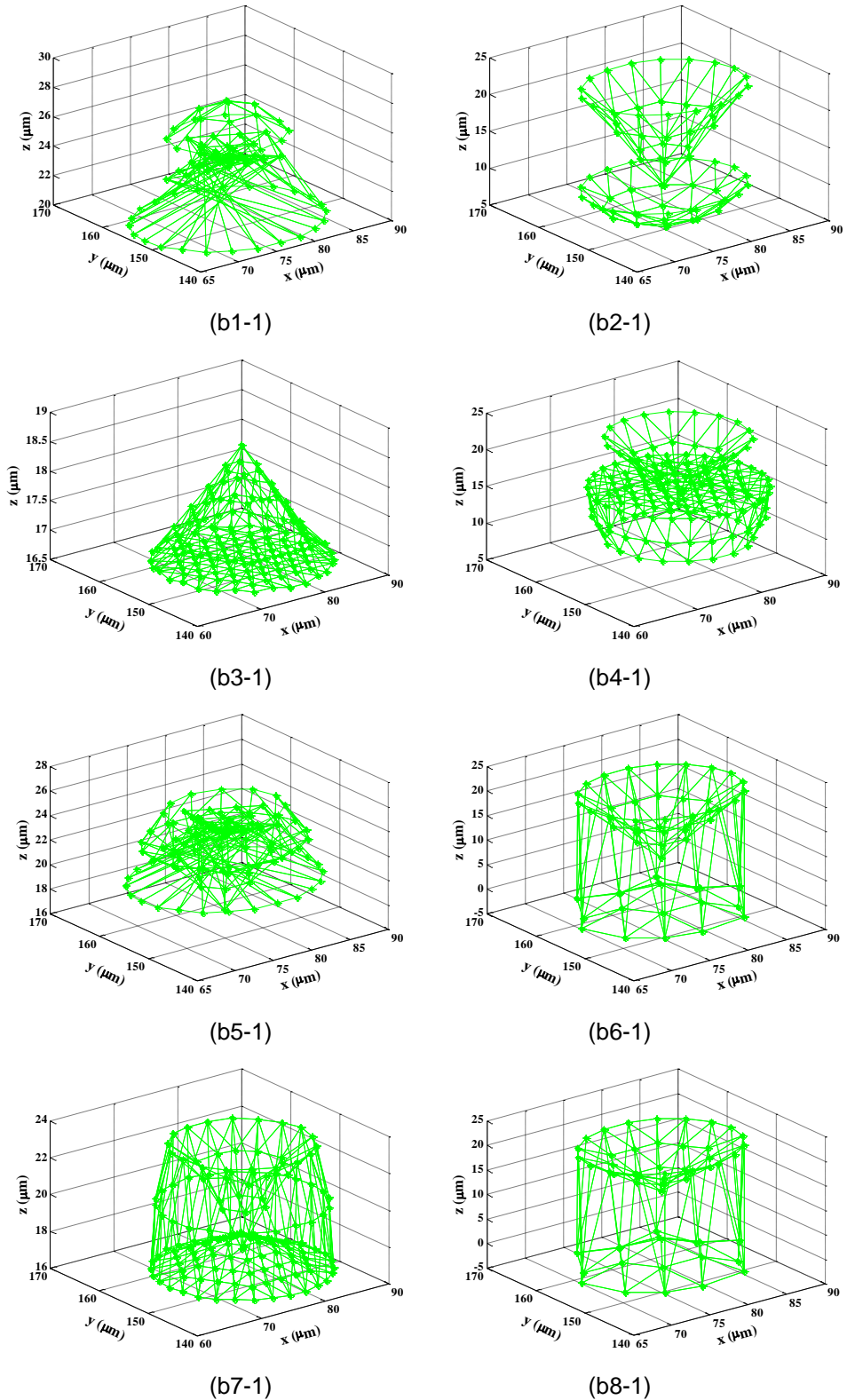


Figure 5. Results of Cleavage Furrow Formation for Eight Cells from the Third Time Division Under 0.08 mM oxygen, 5.5 mM Glucose and 0 mM GIF

In this paper, we omit the results of cell divisions of a tumor cell for the zero time (an initial cell), as shown in Figure 1(a) of paper [15], and for the first time, as shown in Figure 1(b-c) of paper [15], because the related cleavage furrow formations are not needed during these periods of tumor growth. It can be seen that: (1) during the first time division, the initial cell, as shown in Figure 1(a) of paper [15], is divided into two daughter cells after the finite element based growth for four steps (one cell cycle). (2) during the second time division, the tumor cell of Figure 1(b) of paper [15] is divided into cell a1-1 and cell a2-1, while the tumor cell of Figure 1(c) of paper [15] is divided into cell a3-1 and cell a4-1, as shown in Figure 4. Later, these four cells, which are a1-1, a2-1, a3-1 and a4-1, undergo firstly further growths by solving the finite element equations and secondly cleavage furrow formation, with boundaries shown in the black circles from cells of a1-2, a2-2, a3-2 and a4-2, by the proposed approach. (3) during the third time division, each cell of a1-2, a2-2, a3-2 and a4-2 is splitted into two daughter cells according to the black circle boundaries, generating 8 cells which are b1-1 to b8-1, as shown in Figure 5. Compared with the volume based cell division approach which we used in our previous experiments, the cleavage furrow formation based cell division approach is more suitable for the finite element based multi-cellular tumor growth, since the tumor cells are not symmetric and the positions of division planes or cleavage furrows are decided not only chemically but also physically.

6. Conclusion

As one of the most important substances for cytokinesis which is the final act of cell division, the metazoan mitotic spindle determines the position of the cleavage furrow formation. However, we are still unclear about the responsible molecules for these processes. In this paper, we proposed a finite element based cleavage furrow formation approach, which tries to understand the mechanisms of avascular tumor growth not only from the chemical aspect but also from the physical aspect. We also performed several experiments. Results showed that, by using our proposed cleavage furrow formation based cell division approach, the positions of division planes or cleavage furrows are decided not only chemically but also physically and tumor cells are not symmetric, which means our approach is more suitable than our previously volume based cell division approach for multi-cellular tumor growth.

Acknowledgments

This work was supported by the China National Science Foundation under Grants (61201162, 61402106), Basic Research Program of Jiangsu Province (NSF), China (BK2012434), Postdoctoral Research Fund of China (2012M511790), Natural Science Foundation of the Higher Education Institutions of Jiangsu Province, China (12KJB510020), New Teacher Fund for Doctor Station of the Ministry of Education, China (20123223120001) and the Doctor Startup Foundation of Wuyi University under Grant No. 2014BS07. We would like to thank anonymous reviewers for helpful comments.

References

- [1] J. Folkman, "Tumor angiogenesis factor", *Cancer Res.*, vol. 34, (1974), pp. 2109-2113.
- [2] J. X. Chen, et al., "Modeling and performance analyzing of helix transmission base on Modelica," *Key Eng. Mater.*, vol. 455, (2011), pp. 511-515.
- [3] M. A. J. Chaplain, "Avascular growth, angiogenesis and vascular growth in solid tumours: the mathematical modelling of the stages of tumour development," *Math. Comput. Model.*, vol. 23, no. 6, (1996), pp. 47-87.
- [4] C. Y. Liu, "A TPSAC model and its application to mechanical cloud simulation", *Int. J. Secur. Appl.*, vol. 8, no. 1, (2014), pp. 45-56.

- [5] J. P. Freyer and R. M. Sutherland, "Regulation of growth saturation and development of necrosis in EMT6/Ro multicellular spheroids by the glucose and oxygen supply", *Cancer Res.*, vol. 46, (1986), pp. 3504-3512.
- [6] H. Li, "Catalytic hydrothermal pretreatment of corncob into xylose and furfural via solid acid catalyst", *Bioresource Technol.*, vol. 158, (2014), pp. 313-320.
- [7] J. Folkman and M. Hochberg, "Self-regulation of growth in three dimensions", *J Exp. Med.*, vol.138, no. 4, (1973), pp. 745-753.
- [8] H. J. Wang, "Structure design and multi-domain modeling for a picking banana manipulator", *Adv. Mater. Res.*, vol. 97-101, (2010), pp. 3560-3564.
- [9] C. Cabernard, K. E. Prehoda, and C. Q. Doe, "A spindle-independent cleavage furrow positioning pathway", *Nature*, vol. 467, no. 7311, (2010), pp. 91-94.
- [10] J. K. Moon, J. M. Kim, and B. H. Hong, "A study of authentication and access control for library research system", *Int. J. Contr. Autom.*, vol. 7, no. 5, (2014), pp. 235-246.
- [11] P. P. D' Avino, M. S. Savoian, and D. M. Glover, "Cleavage furrow formation and ingression during animal cytokinesis: a microtubule legacy", *J. Cell Sci.*, vol. 118, no. 8, (2005), pp.1549-1558.
- [12] C. Y. Liu, "Study on adaptive and fuzzy weighted image fusion based on wavelet transform in trinocular vision of picking robot", *J. Inf. Comput. Sci.*, vol. 11, no. 6, (2014), pp. 1929-1937.
- [13] R. B. Chalamalasetty, S. Hümmer, E. A. Nigg, and H. H. Silljé, "Influence of human Ect2 depletion and overexpression on cleavage furrow formation and abscission", *J. Cell Sci.*, vol. 119, no.14, (2006). pp. 3008-3019.
- [14] H. L. Li, "One-step heterogeneous catalytic process for the dehydration of xylan into furfural", *BioResources*, vol. 8, no. 3, (2013), pp. 3200-3211.
- [15] C. Liu, "Modeling physical and chemical growths of avascular tumor", *Int. J. Multimed. Ubiqu. Eng.*, vol. 9, no. 4, (2014), pp. 349-362.
- [16] B. Lu, "Discovery of community structure in complex networks based on resistance distance and center nodes", *J. Comput. Inf. Syst.*, vol. 8, no. 23, (2012), pp. 9807-9814.
- [17] J. C. Canman, L. A. Cameron, P. S. Maddox, "Determining the position of the cell division plane", *Nature*, vol. 424, no. 6952, (2003), pp. 1074-1078.
- [18] W. Si, H. H. Gao and X. Y. Li, "A proposed scheme for city family health information system", *Int. J. Smart Home*, vol. 8, no. 3, (2014), pp. 49-60.
- [19] Y. Jiang, "A multiscale model for avascular tumor growth", *Biophys. J.*, vol. 89, no. 6, (2005), pp. 3884-3894.
- [20] H. Li, "A modified biphasic system for the dehydration of D-xylose into furfural using $\text{SO}_4^{2-}/\text{TiO}_2\text{-ZrO}_2/\text{La}^{3+}$ as a solid catalyst", *Catalysis Today*, vol. 234, (2014), pp. 251-256.
- [21] M. Zhou, B. Hu, W. Gao, and J. Wang, "Reinforcement learning fuzzy neural network control for magnetic shape memory alloy actuator", *Int. J. Contr. Autom.*, vol. 7, no. 6, (2014), pp. 109-122.

Authors



Changyu Liu, joined the Communication and Computer Network Lab of Guangdong as a PhD student in 2010 at South China University of Technology, advised by Prof. Shoubin Dong. He was a Visiting Scholar at the School of Computer Science, Carnegie Mellon University, from September 2012 to October 2013, advised by Dr. Alex Hauptmann. Then, he worked with Prof. Mohamed Abdel-Mottaleb at the Department of Electrical and Computer Engineering, University of Miami, from October 2013 to September 2014. His research interests include computer vision and machine learning.



Dapeng Li, he received the B.S. degree in Electronics from Harbin Engineering University, China, in 2003, and the M.S. degree in Communication Systems from Harbin Engineering University, China, in 2006. He received his Ph.D. degree from the Department of Electronic Engineering, Shanghai Jiao Tong University, China, in 2010. From Oct. 2007 to Aug. 2008, he have joined in the 4G/LTE development at the R&D Center, Huawei Company, Shanghai, China. Starting Jan. 2011, he is a faculty

member in the College of Telecommunications and Information Engineering, Nanjing University of Posts and Telecommunications, China. From 03/14-03/15, he is a visiting scholar at University of Miami and Virginia Tech. His research interests include future cellular networks, machine to machine communications, mobile ad hoc networks, cognitive radio networks, radio resource management and cooperative communications.



Bin Lu is currently a lecturer in the School of Computer Science at Wuyi University. He received his Ph.D. degree in 2013 from South China University of Technology. He is a reviewer of the Journal of Yangtze River Scientific Research Institute since 2010. His main research interests include complex network and machine learning.



Tiezhu Zhao received the Ph.D. degree from South China University of Technology in 2011. He is currently a research associate at the Computer College, Dongguan University of Technology. His research interests include distributed/parallel computing, pattern recognition and network security.